SLAC–PUB–7883
July 1998

New Final Focus Concepts at 5 TeV and Beyond*

F. Zimmermann

Stanford Linear Accelerator Center
Stanford University, Stanford, CA 94309, USA

At multi-TeV energies, the length of conventional beam-delivery systems becomes excessive, raising doubts about the value of a compact, high-gradient accelerator to future high-energy physics. In this paper, the reasons for the unfavorable length scaling are discussed, and alternative design concepts are described, for which final focus and collimation systems are orders of magnitude shorter and which produce higher luminosity at lower beam power than conventional approaches. These concepts include a sextupole-free final focus, linac energy-spread compensation, bunch combination and laser collimation. They are compatible with novel acceleration techniques, such as an active matrix linac. A consistent parameter set for a 5 TeV collider is presented.

Invited talk presented at the
8th Workshop on Advanced Accelerator Concepts
Baltimore, Maryland, July 5–11, 1998

*Work supported by the U.S. Department of Energy, contract DE–AC03–76SF00515.

New Final Focus Concepts at 5 TeV and Beyond[1]

Frank Zimmermann

Stanford Linear Accelerator Center
Stanford University
Stanford California 94309

Abstract. At multi-TeV energies, the length of conventional beam-delivery systems becomes excessive, raising doubts about the value of a compact, high-gradient accelerator to future high-energy physics. In this paper, the reasons for the unfavorable length scaling are discussed, and alternative design concepts are described, for which final focus and collimation systems are orders of magnitude shorter and which produce higher luminosity at lower beam power than conventional approaches. These concepts include a sextupole-free final focus, linac energy-spread compensation, bunch combination and laser collimation. They are compatible with novel acceleration techniques, such as an active matrix linac. A consistent parameter set for a 5 TeV collider is presented.

MOTIVATION

It is a striking feature of the proposed design for the 1-TeV Next Linear Collider (NLC) [1] that a third of its length (10 km) is occupied not by the linac, but by the beam delivery system, which consists of collimation section and final focus. For colliders at higher energies the beam delivery system could easily dwarf the linac. A second remarkable feature of the NLC design is that a large portion of the beam power is not converted into luminosity.

FINAL FOCUS

Conventional System

A conventional final-focus system consists of a final telescope, *i.e.*, a few strong focusing quadrupoles producing the small spot at the interaction point (IP), and an upstream chromatic correction section, with sextupole magnets placed at locations of large dispersion generated by bending magnets. Figure 1 shows a schematic of

[1] Work supported by the U.S. Department of Energy under contract DE-AC03-76SF00515.

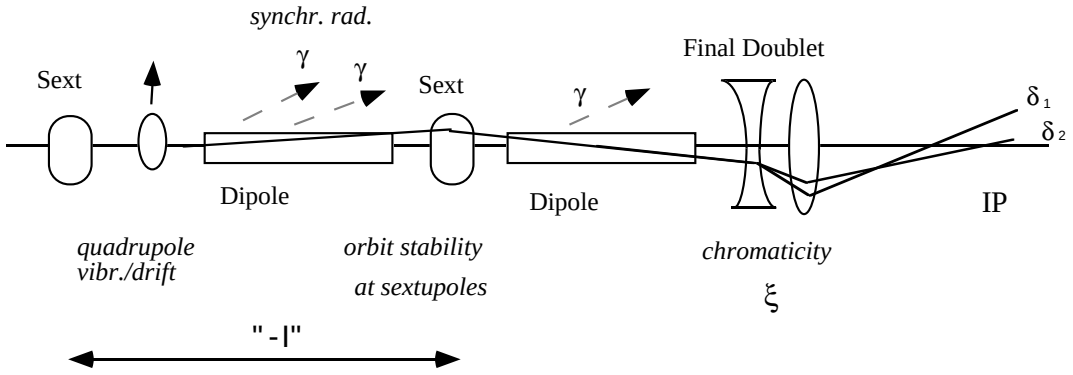

FIGURE 1. Schematic of a conventional final focus.

such a final focus, illustrating its main building blocks and indicating some of the physical processes which dilute the spot size at the interaction point (IP) and give rise to the unfavorable length scaling.

A characteristic property of the final focus is the chromaticity of the last quadrupoles, defined by $\xi = \int K\beta \sin^2\phi \; ds$, where K is the quadrupole strength and ϕ the betatron phase advance to the IP. The chromaticity ξ describes the variation of the focal length with energy. In a conventional final focus, the large chromaticity of the final quadrupoles is compensated by sextupoles in the chromatic correction section. These sextupoles introduce a chromaticity of opposite sign such that particles of different initial energy are focused at the same point. The sextupoles are usually grouped in pairs, separated by an optical $-I$ transform, an arrangement which cancels geometric aberrations. However, this correction scheme is not effective for energy errors generated in the final focus itself: If an additional energy spread is introduced after the first sextupole, the chromaticity of the last quadrupoles is not fully compensated, the focal points for different energies will vary, and the interaction-point spot size will increase.

In the final focus, energy spread is primarily generated by synchrotron radiation in the bending magnets. The higher the beam energy, the weaker and longer the bending magnets of the chromatic correction section must be in order to confine this energy spread. The length l of the final focus is then roughly proportional to the length of the bending magnets, which already in the NLC occupy more than half of the available space. The induced energy spread scales with beam energy γ (energy in units of the rest mass), total bend angle θ_B and length l as [2]

$$\Delta\delta_{\rm rms} \propto \frac{\gamma^{5/2}\theta_B^{3/2}}{l} \qquad (1)$$

As discussed above, energy spread induced in and behind the chromatic correction section increases the IP spot size σ^*. The relative blow-up is given by $\Delta\sigma^*/\sigma^* = \xi\ \Delta\delta_{rms}$, which is added in quadrature to the unperturbed spot size. In a proper design, it is small:

$$\xi\ \Delta\delta_{rms} \ll 1. \tag{2}$$

Next, since the cross section for most reactions decreases inversely with the square of the energy, we assume that, to obtain reasonable reaction rates, the collider luminosity increases as γ^2. If the free length between the interaction point and the last quadrupole as well as the current and the normalized beam emittances are held constant, the chromaticity then increases in proportion to the energy:

$$\xi \propto \frac{1}{\beta^*} \propto \gamma. \tag{3}$$

In addition, the chromatic correction of the final focus for incoming energy errors can be expressed by

$$2\eta_S\ (k_S l_S)\beta_S \approx \xi, \tag{4}$$

where η_S and β_S denote the dispersion and the beta function at the sextupoles, the term $(k_S l_S)$ is the integrated sextupole strength, and the factor of 2 accounts for the two sextupoles of a pair. The ξ is the quadrupole chromaticity defined above. The dispersion η_S in Eq. (4) is proportional to bending angle and system length:

$$\eta_S \propto \theta_B l. \tag{5}$$

A further constraint arises from the orbit stability. Horizontal orbit changes at the second sextupole of a pair, caused by vibrations or position drifts of quadrupoles between the two sextupoles, shift the longitudinal location of the beam waist. This changes the beta function at the collision point, and thereby increases the IP spot size. The achievable orbit stability limits the product of integrated sextupole strength and beta function to

$$(k_S l_S)\ \beta_{S,y} \leq \frac{1}{\Delta x}, \tag{6}$$

where Δx denotes the tolerance on the orbit motion. If we assume that the value of Δx cannot be pushed much below the tolerances assumed in the NLC design [1], combining Eqs. (1)–(6) finally yields the scaling law [3]:

$$l \propto \gamma^2 \tag{7}$$

Thus, the length of a conventional final focus increases roughly as the 2nd power of the energy. Counting both sides of the IP, the length of the 1.5-TeV NLC final focus is 4 km. The final-focus length for a 5 TeV collider would approach 40 km.

Compact Final Focus

The final focus can be made much more compact, if one omits chromatic correction in favor of energy-spread compensation in the linac. This eliminates the long bending magnets and strong sextupoles, as well as the associated tight alignment and stability tolerances on the sextupole orbit. The final focus then consists of quadrupoles only, and can be quite short (one or two hundred meters). Without chromatic correction the incoming beam energy spread must be small: $\delta_{rms} \leq 1/\xi \propto 1/\gamma$. Typical values of ξ for 5 TeV require a relative energy spread smaller than 10^{-5}. For comparison, the present rms energy spread at the end of the SLAC linac is about 8×10^{-4}.

One possibility to attain a smaller energy spread is by employing rf sections operated at harmonics of the fundamental [3]. The energy kick imparted by a linac with such a harmonic acceleration and single-bunch beam loading takes the form

$$V(t) = \sum_h V_h \cos(h\omega_1 t + \phi_h) - \int_0^t dt'\ I(t') W_\parallel(t - t'), \tag{8}$$

with V_h, ϕ_h the voltage and phase for the harmonic h, and ω_1 the angular frequency for the fundamental. The function $W_\parallel$ describes the longitudinal wakefield of the linac and $I > 0$ the bunch current waveform. The total rf input energy per pulse for the harmonic sections relative to that for the fundamental mode rf system is $U_h/U_1 \approx 1/(\rho h^4)$, where ρ is the fractional contribution to the loss factor from the harmonic sections. For $h = 10$ and $\rho = 10\%$, $U_h/U_1 \approx 10^{-3}$.

For the sake of definiteness let us consider a model wakefield, varying with time as $W_\parallel \propto t^{-1/2}$, and a flat-top current profile turning on at $t = 0$ and extending to $t = T$, with $\omega_1 T = 0.2$. The strength of the beam loading is characterized by $\hat{Q} = 1.5\ k_l Q/V_1 \approx 1.3 \times 10^{-2}$, where $k_l = \int_{-\infty}^{\infty} dt\ I(t) \int_{-\infty}^{t} dt'\ I(t) W_\parallel(t - t')$ is the loss factor. In this case, adding a 2nd ($h = 10$) and a third frequency ($h \approx 30$), and optimizing five parameters: fundamental mode phase, harmonic phases and harmonic amplitudes, the energy spread can be reduced to 9×10^{-6} excluding the front 5% of the beam. For this scheme, the pulse-to-pulse intensity fluctuation, $\Delta Q/Q$, must be less than $1/(\hat{Q}\xi) \approx 0.1\%$.

A second method for reducing the energy spread is tailoring the longitudinal bunch distribution [4]. The energy spread along the bunch is reduced to zero, if the bunch distribution $I(t)$ is a solution of

$$I(t) = \frac{\omega_1 V_1}{W_\parallel(0)} \sin(\omega_1 t + \phi_1) - \int_0^t \frac{I(t') \frac{dW_\parallel}{dt}(t - t')}{W_\parallel(0)}\ dt' \tag{9}$$

which can be found numerically. The front of the bunch distribution ($t = 0$) must be sharp edged, with an initial value that depends on the phase ϕ_1: $I(0) = \omega_1 V_1/(W_\parallel(0))\ \sin\phi_1$. If the beam is generated by an rf photo cathode, its longitudinal distribution can be adjusted by manipulating the laser pulse shape.

BUNCH COMBINATION

In addition to its extreme length, a second drawback of the conventional collider layout is that a large portion of the beam power is not converted into luminosity. Due to transverse and longitudinal wakefields in the linac, the beam charge is split into n_b bunches, which are collided separately at a loss in luminosity by a factor of n_b. One can recover some of this luminosity by combining individual bunches into superbunches prior to the collision.

If, for example, the beam consists of bunches propagating in parallel channels, each of small energy spread, but slewed across an energy full width of about 10%—a natural configuration for an active matrix linac [5]—, this combination is easily accomplished. Making use of the energy variation the individual bunches can be combined in a half-chicane, as depicted in Fig. 2. The half chicane consists of two horizontal bending magnets, each of length l_0 and with opposite deflection angles $\pm\theta$ and bending radii $\pm\rho$. The condition for bunch combination is

$$\Delta x = l_0\theta\ \Delta\delta, \tag{10}$$

where Δx denotes the inter-channel distance, and $\Delta\delta$ the bunch-to-bunch energy difference.

The length of the half chicane is determined by synchrotron radiation, inducing an rms energy spread of [2] $\delta_{rms}^2 = 55 r_e \lambda\!\!\!^{-}_c/(12\sqrt{3})\gamma^5\theta^3/l_0^2$, with r_e the classical electron radius and $\lambda\!\!\!^{-}_c$ the Compton wavelength. Since for a compact final focus there is no chromatic correction, this energy spread increases the IP spot size by interacting with the uncompensated final-focus chromaticity ξ. Requiring $\delta_{rms} \leq 1/\xi$, and using Eq. (10), the minimum half length of the half-chicane combiner is

$$l_0 \geq \gamma\ \left(C_\delta \xi^2 \left(\frac{\Delta x}{\Delta\delta} \right)^3 \right)^{1/5} \tag{11}$$

where $C_\delta = 55 r_e \lambda\!\!\!^{-}_c/(12\sqrt{3}) \approx 2.8 \times 10^{-27}$ m^2. If ξ increases in proportion to γ, and the interchannel spacing Δx decreases as $1/\gamma$ (assuming that the linac rf wavelength is decreased inversely proportional to the beam energy), the length l_0 increases as the 4/5th power of energy.

The multi-bunch combination in a half-chicane takes advantage of the different bunch energies, but this energy difference also implies that the optics for each bunch must be matched individually to obtain the same IP beta function. This can be achieved by means of a multi-passband final-focus optics and fine-matching using quadrupole magnets in the still separated beam lines.

COLLIMATION

In general, the beam entering the beam delivery system is not of the ideal shape, but it can have a significant halo extending to large amplitudes, both transversely

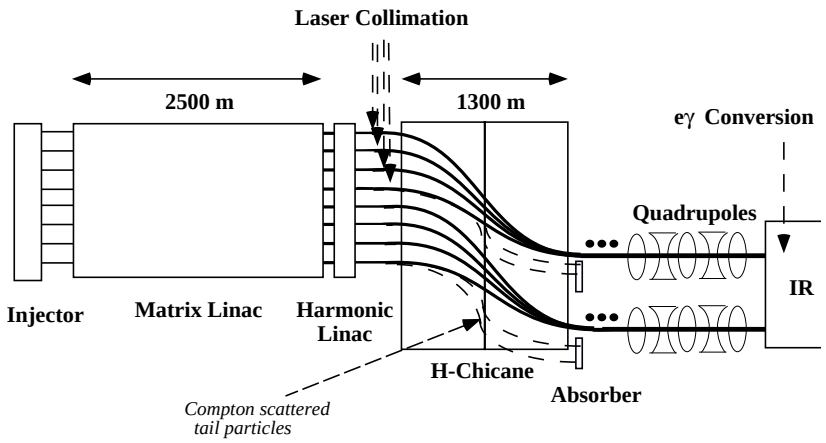

FIGURE 2. Schematic of a 5 TeV collider with linac energy compensation, laser collimation, bunch combination, sextupole-free final focus, and $e\gamma$ conversion.

and longitudinally. There are many sources of beam halo: (1) beam-gas Coulomb scattering, (2) beam-gas bremsstrahlung, (3) Compton scattering on thermal photons, (4) linac wakefields, (5) the source or the damping ring, respectively. The halo generation due to (1) will be reduced by a higher accelerating gradient, while the halo formation due to (2) and (3) scales with the length of the accelerator. The contributions of (4) and (5) to the halo size depend on many parameters; in a first, very rough approximation, if measured as a fraction of the bunch population, they could be considered as constant, independent of energy.

If halo particles hit the beam pipe or a magnet aperture close to the interaction point, they can cause unacceptable background. At the Stanford Linear Collider (SLC), collimation upstream of the final focus was found to be essential for smooth operation and for obtaining clean physics events in the detector. The same is expected to be true for future linear colliders.

Conventional System

A conventional collimation system consists of a series of spoilers and absorbers, which serve two different functions: they remove particles from the beam halo to reduce the background in the detector, and they also protect downstream beamline elements against missteered or off-energy beam pulses. The spoilers increase the angular divergence of an incident beam so that the absorbers can withstand the impact of an entire bunch train [6]. A schematic is shown in Fig. 3.

An important requirement determining the system length is that the collimators have to survive the impact of a bunch train. This requires a minimum spot size, in

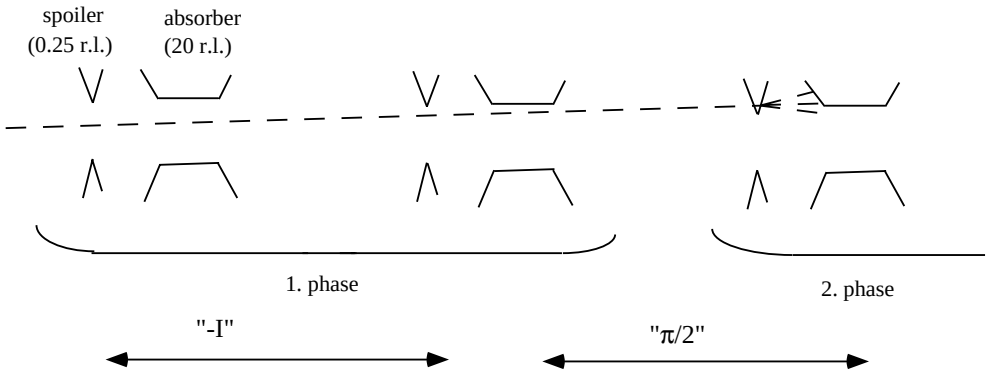

FIGURE 3. Schematic of a conventional collimation system, consisting of a series of spoilers and absorbers. The size of the spoilers and absorbers is approximately 1/4 and 20 radiation lengths, respectively.

order that the collimator surface does not fracture or that the collimator does not melt somewhere inside its volume. For the NLC parameters, fracture and melting conditions give rise to about the same spot-size limit (roughly $10^5/\mu\mathrm{m}^2$ for a copper absorber at 500 GeV [1]). While the surface fracture does not depend on the beam energy, the melting limit does, since the energy of an electromagnetic shower deposited per unit length increases in proportion to the beam energy. Therefore, the beam area at the absorbers must increase linearly with energy. Since, in addition, the emittances decrease inversely proportional to the energy, the beta functions must increase not linearly but quadratically. Assuming that the system length l scales in proportion to the maximum beta function at the absorbers, this results in a quadratic dependence, $l \propto \gamma^2$, *i.e.*, the same scaling as for the final focus. Counting both sides of the IP, the NLC collimation system is 5 km long. At 5 TeV the length of a conventional collimation system could be 50 km.

Laser Collimation

The length of the collimation section can be substantially shortened, if, instead of a solid material, a laser beam is employed as a spoiler. Laser collimation would consist in Compton scattering of particles in the transverse beam tails on a high-power laser beam. At shorter wavelengths also pair production is possible, which would enhance the collimation efficiency. The Compton scattered particles lose a substantial amount of energy, and can be intercepted easily in a dispersive region downstream. Since the energy distribution of the scattered electrons extends over a wide range, the local density of the Compton-scattered part of the beam, which impinges on the energy interceptor, can be very low, without requiring large beta functions in this region. In addition, the laser beam cannot be 'destroyed', and, hence, the beta functions can be much smaller than for a conventional collimator.

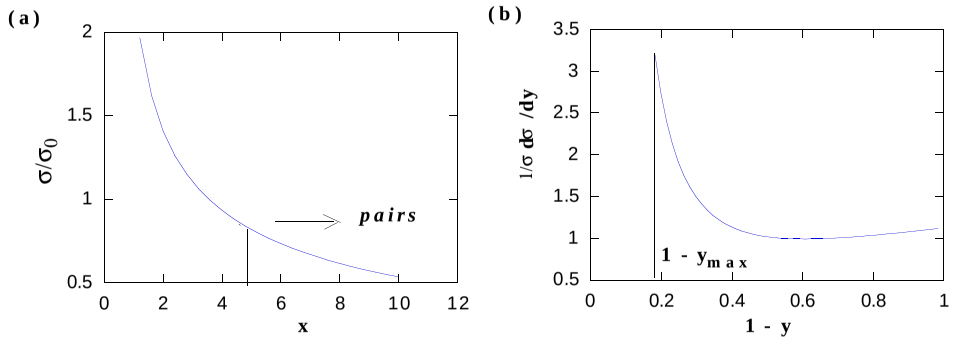

FIGURE 4. (a) Total Compton cross section σ/σ_0 as a function of x; for the scattering of 10-μm photons off a 2.5-TeV electron beam $x = 4.5$. If $x \geq 4.8$, pair production is possible, a regime which should be avoided. (b) Energy spectrum of cross section, $1/\sigma\ d\sigma/dy$, as a function of the fractional scattered-electron energy $E/E_0 = 1 - y = 1 - \hbar\omega/E_0$ for $x = 4.5$, and assuming unpolarized beams. The energy spectrum of the scattered electrons extends from 0 to $1/(1+x)$. The maximum photon energy after scattering is $\hbar\omega_{max} = y_{max}E_0 = x/(1+x)\ E_0$. The cross sections are from Ref. [7].

Indeed, it is advantageous to have a small beta function at the laser spoiler, since this reduces the area to be covered by the laser, and, thereby, also the laser energy needed for efficient collimation. The small beta functions at the spoiler and the large energy spread of the scattered particles suggest that a laser based collimation system could be very short.

The total Compton cross section [7] for an unpolarized photon beam with a few-micron wavelength, scattering off a multi-TeV electron beam, is of the order of the Thomson cross section $\sigma_0 = 2.5 \times 10^{-25}$ cm^2. It is illustrated in Fig. 4 (a) as a function of x. For head-on collisions of laser and particle beam x is given by $x = 4E_0\hbar\omega_0/(m_e^2c^4)$, with E_0 the beam energy and $\hbar\omega_0$ the photon energy. The energy spectrum of the scattered electrons extends from almost unperturbed (100%) to a minimum value of about 20%, as shown in Fig. 4 (b).

To obtain a sharp collimation boundary and to collimate both sides of the beam at once, it is best to use not the fundamental but a higher-order laser mode. The electric field of an arbitrary TEM$_{lm}$ mode is given by [8] $|\hat{E}_{l,m}(x,y,z)| = E_0\ w_0/w(z)\ H_l\left(\sqrt{2}x/w(z)\right) H_m\left(\sqrt{2}y/w(z)\right) \exp\left(-(x^2+y^2)/w^2(z)\right)$ where H_l is the Hermite polynomial of order l, and w is defined by $w^2(z) = w_0^2\ (1 + z^2/Z_R^2)$ with $w_0 = (Z_R\lambda/\pi)^{1/2}$, with Z_R the Rayleigh length, λ the laser wavelength, and z the longitudinal distance from the laser waist. To be specific, let us consider the TEM$_{10}$ mode, for which

$$|\hat{E}_{1,0}| = \sqrt{8}\ E_0 \frac{w_0 x}{w^2(z)}\ \exp\left(-\frac{x^2+y^2}{w^2(z)}\right). \tag{12}$$

The field amplitude E_0 is related to the energy $A_{\rm laser}$ and the total length τ_l of

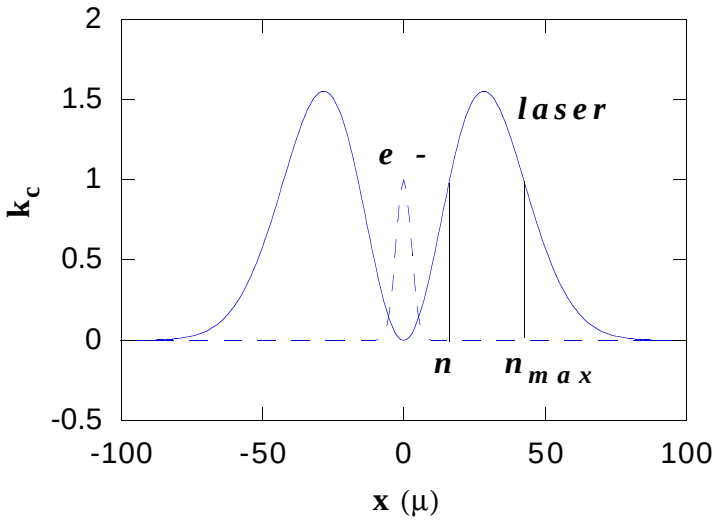

FIGURE 5. Conversion efficiency parameter k_c for Compton scattering of a 5-J 10-μm TEM_{10}-mode laser beam off a 5-TeV electron beam as a function of horizontal position. The beam shape is also indicated by a dashed line. Other parameters are given in Table 2.

the laser pulse via $A_{\mathrm{laser}} = \pi\epsilon_0|E_0|^2\tau_l w_0^2$. The conversion efficiency K_c, *i.e.*, the probability that an electron (or positron) in the beam will Compton scatter, is given by $K_c = 1 - \exp(-k_c)$, where

$$k_c \approx \sigma \frac{dN_\gamma^2}{dx\ dy} = \sigma \frac{\epsilon_0|\hat{E}_{1,0}|^2}{\hbar\omega}\tau_l = \sigma \frac{A_{\mathrm{laser}}}{\hbar\omega w_0^2 \pi}\ \left(\frac{|\hat{E}_{1,0}|^2}{E_0^2}\right). \tag{13}$$

Via $|\hat{E}_{1,0}|^2$, it is a function of the transverse position. For a TEM_{10} mode, the conversion efficiency is zero at the center of the laser beam, then increases quadratically, and falls off at large amplitudes like a Gaussian with an rms width $w(z)/2$. If the laser intensity is high enough, k_c is equal to 1 at two different amplitudes. The smaller of these amplitudes may be considered as the effective collimation depth, the larger one as the maximum amplitude which is still collimated. We denote these two amplitudes, in units of the rms beam size, by n and n_{max}, respectively. The position dependence of k_c is illustrated in Fig. 5.

Even if the particle beam is of purely Gaussian shape and is well-centered in the node of the laser field, there is an unavoidable fraction of particles that is lost due to Compton scattering. For a collimation depth n this fraction is

$$\frac{\Delta N_b}{N_b} \approx \frac{1}{n^2} \tag{14}$$

where N_b is the bunch population. For example, if we collimate at $35\sigma_x$ ($n \approx 35$) less than 10^{-3} of the particles in the centered Gaussian beam core are scattered, while at $6\sigma_x$ the scattered fraction would be 3% (per plane).

If the laser collimation is situated at the end of the linac, the scattered tail particles, which are off energy, can be intercepted downstream of the bunch-combining half chicane (see Fig. 2), where the dispersion is nonzero, $\eta = \theta l_0$. The density of the scattered particles must stay below the melting limit of the absorbing material: $N_b/(\sigma_x\sigma_y) \leq n_{\rm limit}/\gamma$, where $n_{\rm limit} \approx 10^{12}/\mu{\rm m}^2$. The horizontal size of the Compton-scattered beam at the absorber is determined by the rms energy spread of the scattered particles, δ_C ($\delta_C \approx 0.1$), and by the dispersion, η, as $\sigma_x \approx \eta\delta_C$. The vertical size follows from the angular spread of the scattered particles, $y'_{\rm rms} \approx 1/\gamma$, and the length of the combiner: $\sigma_y \approx 2l_0/\gamma$. Combining these equations with the constraint on the energy spread induced by synchrotron radiation, $\delta_{rms} \leq 1/\xi$, we derive a lower limit on the combiner half length l_0 which guarantees survival of the absorber, even if the entire electron beam is missteered and Compton scattered:

$$l_0 \geq \gamma^{11/8}\ N_b^{3/8}\ \xi^{1/4}\ \left(C_\delta \frac{1}{\delta_C^3 n_{\rm limit}^3}\right)^{1/8} \approx\ 10^{-12}\ [{\rm m}]\ \gamma^{11/8}\ N_b^{3/8}\ \xi^{1/4} \qquad (15)$$

For the 5-TeV parameters discussed below, this limit is a factor 6 shorter than the minimum combiner length of Eq. (11). So it is automatically fufilled. If on the other hand the laser is located behind the combiner and off-energy scattered particles are to be absorbed in a dedicated full chicane downstream, the total length of that chicane would be 4.4 l_0 with l_0 as given in Eq. (15).

5-TEV COLLIDER

As an illustration, we now consider the beam delivery system for a 2.5-TeV parallel-beam accelerator operating at W-band (91 GHz) [5]. The linac consists of a primary energy storage line running parallel to the beam axes, secondary lines running roughly orthogonal to the beam axes, and a switch coupling between the lines every 1/3 of a wavelength, all as depicted in Fig. 6. The temporally coincident beams propagate in parallel channels, spatially separated by $\Delta x = 1.4$ mm.

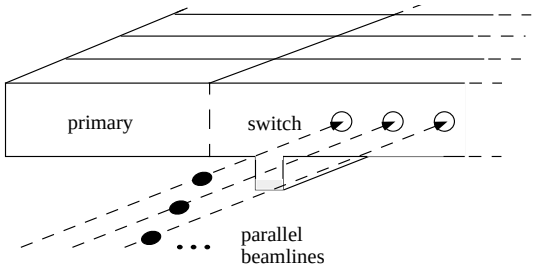

FIGURE 6. The linac employs a 'primary' storage line, a switch and a series of secondary transmission lines [5].

We assume that the two colliding beams consist of 50 bunches with a charge of 60 pC each, and with transverse emittances of $\gamma\epsilon_{x,y} \approx 100$ nm, as could be produced

by an advanced rf gun. The rms bunch length is chosen as about 10 μm. These and other beam parameters are compiled in Table 1.

A relative energy spread across each bunch smaller than 10^{-5} is achieved either by harmonic acceleration, or bunch shaping, or a combination thereof. For example, harmonic acceleration could employ the 10th and 30th harmonic of the fundamental frequency, where the 10th harmonic (0.91 THz) might be provided by a 100-m matrix rf section with a gradient of 200 MeV/m. The $h = 30$ (2.7 THz) section would correspond to a 1-m plasma linac at the linac exit, with a plasma density of $n_e \approx 10^{17}$ cm^{-3} and a 'modest' accelerating gradient of about 3 GV/m.

Behind the linac, groups of 10 bunches are combined into superbunches, for higher luminosity. Assuming a 1% energy difference $\Delta\delta$ between adjacent channels, the minimum length of the bunch-combining half chicane, Eq. (11), is $2l_0 \geq 1300$ m.

The laser collimation can be performed at two different locations. The first possibility is to place the laser at the end of the linac and to intercept the Compton scattered electrons after the 1.3-km long bunch combiner, where the dispersion is nonzero. The second possibility is to install the laser behind the combiner, in which case an additional bending section downstream is required, for example a 500-m long full chicane, where a collimator can intercept the scattered off-energy particles. The second option would simplify the laser system, by reducing the number of laser pulses, but it would increase the system length. Sample laser and beam parameters, applicable for either option, are listed in Table 2. A CO_2 laser fulfilling all the requirements is considered within the reach of the CO_2 laser technology [9].

The final-focus optics must have a multiple-energy passband, individually matched for each accelerating channel. Fig. 7 shows 3 matched beta functions over the last 80 m prior to the IP, spanning a total energy range of 10%, with initial optical functions (on the right) identical to the FODO lattice at the end of the linac. In Fig. 7 a series of final-focus quadrupoles were adjusted to obtain the same IP beta function for each energy. For perfect matching the optics can be fine-tuned using quadrupoles in the linac, where the bunches are still separated.

For the assumed emittances, an IP free length of $l^* = 2$ m and a maximum final quadrupole strength of $K \approx 1$ m^{-2}, the effect of synchrotron radiation in the final two quadrupoles (Oide effect) [10] limits the IP spot size in both planes to about 1.7 nm. Monte Carlo simulations show that, for this spot size, the ideal luminosity is reduced by about 20%. This factor increases rapidly, when the IP beta functions are lowered further.

Synchrotron radiation in the other final-focus quadrupoles is not an issue: At a beam energy of 2.5 TeV, each electron radiates about $dN_\gamma/ds \approx 5/(3\sqrt{2})\alpha\gamma K\sigma_{x,y} \approx 6\times10^{-3}[\mathrm{m}^{1/2}]\ K\sqrt{\beta_{x,y}}$ photons per unit length, with K the quadrupole gradient (in m^{-2}), $\sigma_{x,y}$ the rms beam size and $\beta_{x,y}$ the beta function (both in m), and assuming emittances of $\gamma\epsilon_{x,y} \approx 100$ nm. For $K \approx 0.5$ m^{-2}, $\beta_{x,y} \approx 10$ km, and a length of 60 m, this amounts to $N_\gamma \approx 18$ photons per electron, a sizable number, but the critical relative photon energy is only $\delta_c \approx 1.5\lambda\!\!\!^{-}_c K\sigma_{x,y}\gamma^2 \approx 2\times10^{-8}[\mathrm{m}^{3/2}]\ K\sqrt{\beta_{x,y}} \approx 10^{-6}$,

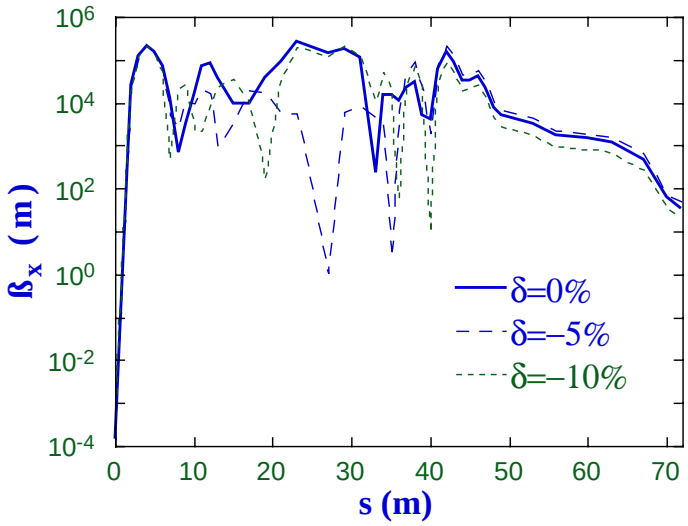

FIGURE 7. Final-focus beta functions for 10% different beam energies; on the right are linac-like FODO cells with $\beta \approx 20$ m, on the left the IP with $\beta = 150$ μm.

a factor of 10 smaller than the final-focus energy bandwidth.

Finally, during the collision, particles emit synchrotron radiation in the field of the opposing beam. The strength of this 'beamstrahlung' is characterized by the parameter Υ, which is proportional to the average critical energy, $\Upsilon \approx 5\gamma {r_e}^2 N_b/(6\alpha\sigma_z(\sigma_x + \sigma_y))$, where $\alpha \approx 1/137$ is the fine structure constant, and σ_z the rms bunch length. For the parameters of Table 1, $\Upsilon \approx 500$, implying an enormous energy loss per electron, a large number of photons per electron, and coherent pair production as the dominant background source. Two possible remedies are: $\gamma\gamma$ collisions and charge compensation.

$\gamma\gamma$ Collisions

Photon-photon collisions are a very attractive option for a 5-TeV high-luminosity collider, because of two reasons: (1) there is no luminosity degradation and no background due to beamstrahlung, and (2) unpolarized low-current electron beams with the required emittances in both tranverse planes may be produced by advanced photocathode rf guns.

Photon-photon collisions are realized by converting the 2.5-TeV electrons into high-energetic photons via Compton scattering on a high-power laser beam [11]. The laser parameters are very similar to those assumed for collimation. The optimum laser wavelength with regard to conversion efficiency and photon energy spectrum depends on the beam energy as [7] $\lambda = 4.2\ E_0[\mathrm{TeV}]\ \mu$m. At a beam energy E_0 of 2.5 TeV, the required wavelength is about 10 μm; this corresponds to a CO_2 laser. After conversion the photon beam diverges as $1/\gamma$. This lim-

its the maximum distance b between conversion point and collision point (CP) to $b \leq \sigma^*_{x,y}/(2\gamma) \sim 5$ mm, where $\sigma^*_{x,y}$ denotes the electron-beam spot size without Compton scattering.

To obtain a reasonable conversion efficiency of 65% or higher, the laser energy flux per pulse must exceed $I\tau_l \geq \hbar\omega/\sigma \sim 10^5$ Ws/cm^2, where I denotes the intensity (in W/cm^2), τ_l the laser pulse length, and σ the Compton cross section.

If the laser density is too high, multiphoton processes occur, and, at the same time, the maximum photon energy acquired in a single photon process is reduced [7,12]. For this reason, the laser intensity I for a 10 μm wavelength should be smaller than $I \leq 10^{16}$ W/cm^2. Combined with the above limit on $(I\tau_l)$ this requires a total laser pulse length of $\tau_l \geq 10$ ps (or $c\tau_l \geq 3$ mm).

The Rayleigh length should not be much shorter than the pulse length, *e.g.*, $R_L \approx 1$ mm. The transverse laser extent $w_0 \approx (\lambda Z_R/\pi)^{1/2} \approx 56$ μm then determines the energy of the laser pulse: $A \approx I\tau_l w_0^2 \pi/2 \approx 5$ J. The divergence of the laser light, $\alpha_\gamma \approx \lambda/(2\pi w_0)$, and a typical damage threshold for mirror materials of 1 J/cm^2, yield the minimum focal distance of the last mirror: $F \geq (A_{\rm laser} 2\pi w_0^2/\lambda^2/(1{\rm J/cm}^2))^{1/2} \approx 30$ cm. Finally, the F-number 'FN', defined as the ratio of focal length and incoming laser-beam diameter, relates the wavelength and the spot size at the focus: $w_0 \approx 2.4\lambda\, FN$. For our example, FN is 2, a realistic value. Parameters relevant to $e\gamma$ conversion are summarized in Table 2.

Charge Compensation

An alternative to photon-photon collisions is the suppression of beamstrahlung via charge compensation [13]. Here electron and positron bunches are combined into neutral bunches, prior to the collision. Since the net charge is greatly diminished (ideally there is none), the electromagetic fields and, hence, the beamstrahlung can be reduced by orders of magnitude. However, if the two oppositely charged bunches are initially offset with respect to one another, a charge-separation instability can develop [13,14]. For a single collision point, this effect was analyzed both analytically and by a computer simulation [15]. For the moderate collision strength considered here, with disruption parameters $D_{x,y} = 2N_b r_e \sigma_z/(\gamma\sigma^\star_{x,y}(\sigma^\star_x + \sigma^\star_y)) \approx 9$, this instability is not a problem.

CONCLUSIONS

Extrapolation of present-day final-focus and collimation systems to higher energies results in excessive site length and beam power. In this report, we have outlined an alternative design concept, which provides for a much shorter system length and for higher luminosity at lower beam power than the conventional approach. This concept was illustrated by means of a sample design for a 5-TeV $\gamma\gamma$ collider, whose parameters are summarized in Table 1. The proposed collider achieves a $\gamma\gamma$ luminosity of 1.5×10^{34} cm^{-2}s^{-1} for an average beam power as low as

TABLE 1. Parameters for a 5-TeV $\gamma\gamma$ collider.

variable	symbol	value
beam energy	E_0	2.5 TeV
particles per superbunch at CP	N_b^*	3.8×10^9
number of superbunches	n_b^*	5
number of linac bunches	n_b	50
charge per linac bunch	Q	60 pC
repetition frequency	f_{rep}	120 Hz
average beam power (per side)	P	0.9 MW
rms linac energy spread	δ_{rms}	10^{-5}
rms bunch length	σ_z	10 μm
transverse emittance	$\gamma\epsilon_{x,y}$	100 nm
IP spot size w/o Oide effect	$\sigma_{x,y}^*$	1.7 nm
IP beta function	$\beta_{x,y}^*$	150 μm
$\gamma\gamma$ luminosity w. 65% conversion efficiency	$L_{\gamma\gamma}$	1.5×10^{34} cm^{-2}s^{-1}

TABLE 2. Parameters for laser collimation and $e\gamma$ conversion.

variable	symbol	value (collimation)	value ($e\gamma$ conversion)
laser energy / pulse	$A_{\rm laser}$	5 J	5 J
laser wavelength	λ	10 μm	10 μm
Compton scattering parameter	x	4.5	4.5
laser pulse length	τ_l	2 ps	10 ps
laser mode TEM	(l,m)	(1,0)	(0,0)
laser parameter	w_0	40 μm	56 μm
laser Rayleigh length	Z_R	500 μm	1 mm
laser intensity	I	10^{17} W/cm^2	10^{16} W/cm^2
min. focal distance of last mirror	F	16 cm	30 cm
number of photons / pulse	N_γ	2.7×10^{20}	2.7×10^{20}
rms beam size at laser IP	$\sigma_{x,y}$	2.7 μm	N/A
beta function at laser IP	$\beta_{x,y}$	365 m	N/A
collimation depth	$n_{x,y}$	6	N/A
collimation limit	$n_{max,\ x,y}$	16	N/A
fraction of 'core' scattered	$\Delta N_b/N_b$	6%	N/A
rms beam size at $e\gamma$ CP	$\sigma_{x,y}$	N/A	60 nm
distance between $e\gamma$ CP and IP	b	N/A	5 mm
conversion efficiency	K_c	N/A	65%

0.9 MW. A beam power of 6 MW would yield a luminosity of 10^{35} cm^{-2}s^{-1}. The total collider length is less than 10 km.

ACKNOWLEDGEMENTS

I am grateful to David Whittum for many of the ideas, and to John Irwin, Tor Raubenheimer and Dick Helm for sharing their insights into linear-collider final-focus and collimation systems. I thank Theo Kotseroglou for confirming the feasibility of the laser parameters.

REFERENCES

1. "Zeroth Order Design Report for the Next Linear Collider," *SLAC-Report* **474** (1996).
2. M. Sands, "The Physics of Electron Storage Rings," *SLAC*-**121** (1979).
3. F. Zimmermann and D.H. Whittum, "Final-Focus System and Collision Schemes for a 5-TeV W-Band Linear Collider," in *Proc. of 2nd Int. Workshop on e^-e^- Interactions at TeV Energies, Santa Cruz 1997*, and *SLAC-PUB*-**7741** (1998).
4. G.A. Loew and J.W. Wang, "Minimizing the Energy Spread with a Single Bunch by Shaping its Charge Distribution," *IEEE Trans. Nucl. Sc.*, **32**, no. 5 (1985).
5. D. Whittum and S. Tantawi, "Active Millimeter-Wave Accelerator with Parallel Beams," subm. to *Phys. Rev. Lett.* (1998).
6. H. DeStaebler, D. Walz, and J. Irwin, in Ref. [1].
7. V. Telnov, "Principles of Photon Colliders", *Nucl. Instr. Methods A* **355**, 3 (1995).
8. A. Yariv, "Quantum Electronics", Wiley (1976).
9. I. Pogorelsky, "Terawatt Picosecond CO_2 Laser Technology for Future TeV Colliders", submitted to *Laser and Particle Beams*, *BNL*-**64281** (1997).
10. K. Hirata, K. Oide, B. Zotter, "Synchrotron Radiation Limit of the Luminosity in TeV Linear Colliders," *Phys. Lett. B224*, **437** (1989).
11. I. Ginzburg, G. Kotkin, V. Serbo, V. Telnov, "Colliding γe and $\gamma\gamma$ Beams based on the Single-Pass e^-e^- Colliders (VLEPP type), *Nucl. Instr. Methods A* **205**, 47 (1983).
12. K.J. Kim it et al., "A Second Interaction Region for Gamma-Gamma, Gamma-Electron and Electron-Electron Collisions for NLC", in Ref. [1] and *LBNL*-**38985** (1986).
13. V.E. Balakin and N.A. Solyak, *Proc. XIII Int. Conf. on High Energy Accelerators*, Novosibirsk, USSR, p. 151 (1986).
14. J.A. Rosenzweig, B. Autin and P. Chen, *Proc. 1989 Lake Arrowhead Workshop on Advanced Accelerator Concepts*, p. 324 (1989).
15. D.H. Whittum and R.H. Siemann, "Neutral Beam Collisions at 5 TeV," in *Proc. of IEEE PAC97 Vancouver* (to be published).